

# A model for Magnetic Actuation of the Artificial Multicilia

Semih Özel <sup>1</sup>, Daniel IOAN <sup>2</sup>, Mihai Rebican <sup>3</sup>

<sup>1</sup>Dept. of Electrical and Electronics, Engineering Faculty,  
Marmara University, Turkey  
[semih.ozel@marmara.edu.tr](mailto:semih.ozel@marmara.edu.tr)

<sup>2</sup>Dept. of Electrical Engineering, Numerical Methods Laboratory,  
University Politehnica of Bucharest, Romania,  
[daniel@lmm.pub.ro](mailto:daniel@lmm.pub.ro)

<sup>3</sup> Dept. of Electrical Engineering, Numerical Methods Laboratory,  
University Politehnica of Bucharest, Romania,  
[mihai\\_r@lmm.pub.ro](mailto:mihai_r@lmm.pub.ro)

## Abstract

The current paper continues the analysis of a completely novel method of fluid manipulation technology in micro-fluidics systems, inspired by nature, namely by the mechanisms found in ciliates. More information on this subject can be found at <http://www.hitech-projects.com/euprojects/artic/>. The paper presents a fast and accurate method to model the magnetic behavior of an artificial cilium. The method is based on Maxwell equations, formulated as integral equations for the magnetization. Also this paper consists on assessing magnetic actuation as a practical tool for obtaining a consistent one-directional fluid flow. The actuation mechanism consists of a bi-directional rotating excitation magnetic field. The magnetization induced by the magnetic field was calculated in a separate routine based on the Integral Nonlinear Equations Approach with 1D discretization of wire (cilium). Time averaged x-coordinate mass flow rates are computed for several cilium configurations resulting.

## 1. Introduction

The on-going miniaturization in a variety of scientific domains especially biochemistry and medicine requires manipulation of smaller and smaller volumes of biological fluids such as blood, saliva, urine, or polymer solutions. Examples of such applications are micro-channel cooling for electronics, inkjet printing for displays and biomedical applications, controlled drug delivery systems and biosensors. Also, the nature of the manipulation may be quite broad: transportation, mixing, sorting, deforming, or rupturing. An attractive solution in part fulfillment of these goals is represented by artificial cilia arrays. Cilia are thin hair-like cell appendices responsible for many essential biological functions. One of the most interesting and useful cilia functionalities is propulsion, meaning either self-propulsion of the organism or inducing fluid flow around a stationary organism at micron-scale dimensions. Theoretical research in this domain has mainly been devoted to understanding the biochemical engine driving such complex movements and providing valuable insights of the interaction between the deformations of the elastic structure and the viscous incompressible fluid surrounding it [1, 2, 3, 4]. Based on their typical dimensions and physical properties of

biological fluids we are able to assess that the Reynolds number of such flows is of the order of unity or less. In this case not only the flow is laminar but it is dominated by viscous forces that make it close to a classical Stokes flow. On the other hand, the dynamics of such elastic structure lacks the inertial term because of the very small characteristic mass. The movement of the individual cilia is asymmetric, i.e. a deformation cycle consists of an effective stroke and a recovery stroke. During the effective stroke the cilium behaves like a rigid rod while in the recovery stroke it bends and rolls back to the original position so that a resultant fluid transport in one direction is induced. Also, cilia operate collectively by hydrodynamic interaction that induces mutational coordination, a slight phase lag of their movements generating wave-like aspect. Such behavior seems to aim at reducing energy expenditure per cycle beat.

Inducing sustainable one-direction flow with artificial cilia has several distinctive features comparing to the biological counterpart. The main issue is the different way of attaching the cilium to the support substrate. Contrary to the upright position of the natural cilium, the artificial one was tilted towards horizontal plane. The tilt angle may vary between 0 and 10-20 degrees. A flow efficiency analysis has showed better performance for an asymmetric geometric shape of the cilium associated with a harmonic actuation mechanism [5]. In the present paper we are proposing to fast and accurate method to model the magnetic behavior of the artificial cilium. The movement of the artificial cilia can be actively controlled, preferably using a magnetic field or an electrical field [6]. In this method, integral equations of the electrical and magnetic field are described. Rest of paper consists of investigating the main fluid flow features of an array of artificial cilia in a semi-infinite domain. As in the previous case [5], the actuation mechanism consists of a bidirectional rotating excitation magnetic field that interacts with the magnetized cilium. Velocity fields and lateral boundaries mass flow rates are computed for several cilia array configurations.

## 2. Physical model

The cilium is modeled as an inextensible cylindrical filament of length  $L$  and circular cross section of radius  $a$ . The slenderness of the cilium is defined by ratio  $\epsilon = a / L \ll 1$ . The center line of the filament is parameterized by its arc-length  $s$  ( $0 \leq s \leq L$ ). The null value corresponds to the anchor point where

the cilium is attached to the substrate surface;  $s = L$  at the distal end. Two coordinate systems (CS) are defined, one fixed at the anchor and a Lagrangean one attached to an arbitrary point on the cilium. Due to the axial symmetry in the magnetic field density we shall restrict our analysis to planar case. Hence, the coordinate systems are  $(x,y)$ , global, and  $(T,N)$ , local. The angle between the tangential direction in local CS and the  $x$  axis in global CS for each cilium in the array of  $K$  cilia is denoted  $\alpha^{(k)}$ ,  $k = 1, \dots, K$ , being a function of arc-length, time and  $\alpha^{(k)} = \alpha^{(k)}(s, t)$ . The parameterized equations of the center line points are given by

$$x^{(k)}(s, t) = \int_0^s \cos(\xi^{(k)}, t) d\xi^{(k)} + x_0^{(k)},$$

$$y^{(k)}(s, t) = \int_0^s \sin(\xi^{(k)}, t) d\xi^{(k)} \quad (1)$$

where  $x_0^{(k)}$  stands for the abscissa origin of each cilium of the array. The driving engine is represented by the magnetic torque  $C^{(k)} = C^{(k)}(s, t)$ . The response from the elastic structure is denoted by the shear force  $\bar{F}^{(k)} = F^{(k)}(s, t)$  and  $\varphi^{(k)} = \varphi^{(k)}(s, t)$  are the viscous forces per unit length (drag forces) exerted by the surrounding fluid. Here and in the following the bold typeface denotes vector quantities. The velocity of the current cross section  $s$  of the arbitrary cilium  $(k)$  in the array is denoted by  $V^{(k)} = V^{(k)}(s, t)$ . From the mechanical point of view, we consider that each cilium is in mechanical equilibrium at every moment of time.

## 2.1. Equations of motion.

Considering a finite volume of an arbitrary cilium along the arc-length  $ds$  the balance of forces and moments in the local Frenet coordinate system reads:

$$\boldsymbol{\varphi}_N^{(k)} = F_{N,s}^k + F_T^{(k)} \boldsymbol{\alpha}_s^{(k)} \quad (4)$$

$$\boldsymbol{\varphi}_T^{(k)} = F_{T,s}^k + F_N^{(k)} \boldsymbol{\alpha}_s^{(k)} \quad (5)$$

$$C_{m,s}^{(k)} + F_N^{(k)} = EI \boldsymbol{\alpha}_{ss}^{(k)} \quad (6)$$

where subscripts  $N, T$  means normal and tangential components and  $s, t$  denote arclength and time derivation.  $C_{m,s}$  is the derivative of the magnetic torque. The drag force components are specified through linear dependence on velocity components

$$\boldsymbol{\varphi}_N^{(k)} = -C_N V_N^{(k)} + \boldsymbol{g}_N^{(k)} \quad (7)$$

$$\boldsymbol{\varphi}_T^{(k)} = -C_T V_T^{(k)} + \boldsymbol{g}_T^{(k)} \quad (8)$$

$$\boldsymbol{g}_N^{(k)} = C_N \boldsymbol{G}_N^{(k)} \quad \boldsymbol{g}_T^{(k)} = C_T \boldsymbol{G}_T^{(k)} \quad (9)$$

where  $\boldsymbol{G}_N^{(k)}$  and  $\boldsymbol{G}_T^{(k)}$  are the local CS components of the velocity induced at current location by the flow field generated by superposition of Stokes equation fundamental solutions and their image systems [2]. The normal and tangential specific drag coefficients are denoted by  $C_N$  and  $C_T$ . Time differentiation of geometrical relations (1) leads to kinematic conditions:

$$V_{N,s}^{(k)} = \boldsymbol{\alpha}_t^{(k)} - V_T^{(k)} \boldsymbol{\alpha}_s^{(k)} \quad (10)$$

$$V_{T,s}^{(k)} = V_N^{(k)} \boldsymbol{\alpha}_s^{(k)} \quad (11)$$

## 3. Integral equations method

Let us consider the cilium as a linear magnetic wire with a rectangular cross section placed in a uniform magnetic field (Fig. 1). Using a magnetic field computation, the magnetic flux density, torque and force in the cilium are obtained.

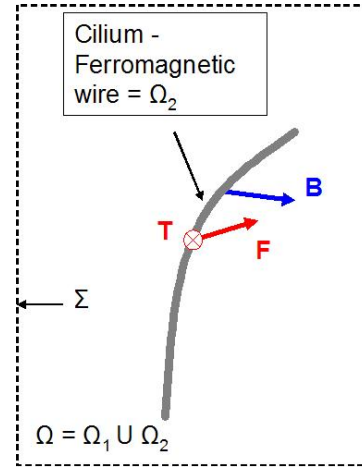


Fig. 1. Computation domain of the cilium

Starting from the Maxwell equations, the integral equation for magnetization is:

$$\boldsymbol{M} + \frac{\chi}{4\pi} \int_{\Omega_2} \frac{R \operatorname{div} \boldsymbol{M} dv}{R^3} = \chi \boldsymbol{H}_0 + \boldsymbol{M}_p \quad (12)$$

where  $\boldsymbol{H}_0$  is the external magnetic field.

The cilium is divided in  $n$  segments (1D finite elements), and each parallelepiped element is uniformly magnetised along the cilium direction (Fig. 2). Using this assumption, (1) becomes a linear system of  $n$  equations [7].

$$M_j + \frac{\chi g \Delta z}{4\pi} \sum_{i=1}^n \left[ \frac{M_i \cos(\Delta\beta_i/2) - M_{i-1} \cos(\Delta\beta_i/2)}{a_{ij} \sqrt{(\Delta z/2)^2 + a_{ij}^2}} \right] = \chi H_0 + M_p, \quad j = 1, n \quad (13)$$

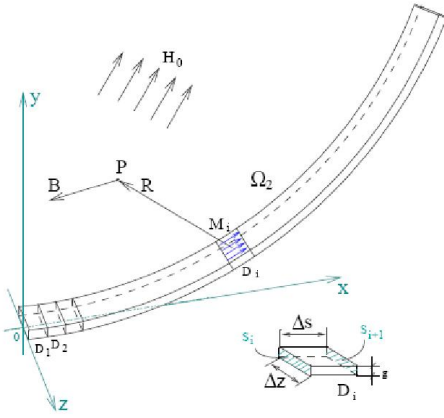


**Fig. 2.** Discretization of the cilium for the magnetic field computation

(Fig. 3) shows the magnetic flux density along a right cilium, which is discretized in 10 finite elements. The cilium ( $\mu_r = 100$ ) is situated into a uniform magnetic field ( $B_0 = 10$  mT), oriented along the cilium. The cilium has parallelepiped geometry ( $100 \times 20 \times 2 \mu\text{m}$ ).

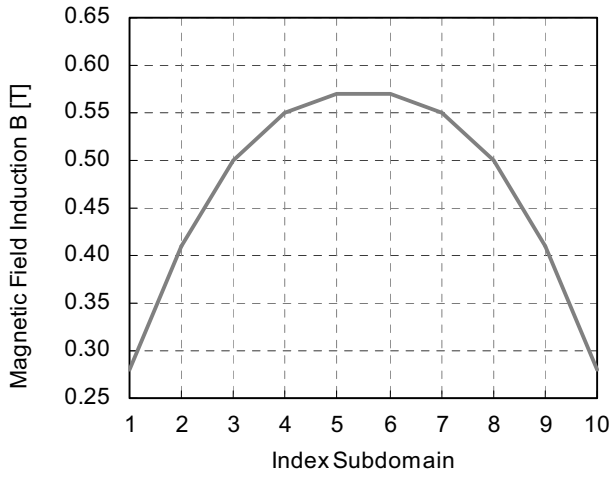


**Fig. 3.** Magnetic flux density along a straight cilium situated in a uniform magnetic field

The details of this method and more numerical results for different test cases of the cilium will be presented in the full paper.

#### 4. Numerical approach

The derivative of magnetic torque used in the equilibrium condition (4) provides the active force denoted by

$$S = \frac{dC_m}{ds} \quad (14)$$

After proper non-dimensionalization a system of integro-differential equations has to be solved in order to account for the fluid structure interaction [2, 5]. Based on an adequate linear discretization of the arc-length of each wire (31 segments, for example) and using a Crank-Nicholson finite difference scheme, the system is solved for the time-depending parameterization of the array of artificial cilia  $\alpha^{(k)} = \alpha^{(k)}(s, t)$ . The same boundary as in [5] is imposed. As for initial conditions, we have

$$\alpha^{(k)}(0, 0) = \pi/18$$

$$\alpha^{(k)}(s, 0) = \frac{\pi}{18} + \frac{\pi}{18(N-1)} \left( 10.5 - s \frac{N}{L} \right)$$

$$\text{for } s > 0 \quad (15)$$

a typical discretization of the fluid domain surrounding the cilium using a rectangular grid is depicted in (Fig. 4).

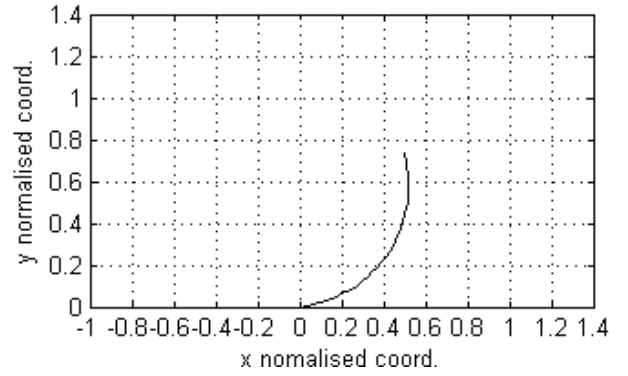


**Fig. 4.** Geometry and grid.

The velocity field  $\mathbf{V}(v_x, v_y)$  in this domain is calculated based on the singular solution of Stokes equation (Stokeslet) for all nodes of the grid  $(x_g, y_g)$

$$\mathbf{V}(x_g, y_g, t) =$$

$$= \sum_{k=1}^K \int_{0 \leq s \leq L} U_s(R(x_g, y_g), R^{(k)}(s, t), -\phi^{(k)}(s, t)) ds \quad (16)$$

Using this velocity field we are able to determine the x-coordinate mass flow rate generated by the magnetic actuation of the cilium in every section  $x = ct$  of the domain.

$$\dot{m}_x = L \rho_w \int_{y=0}^{y=1.5} v_x dy \quad (17)$$

where  $\rho_w$  is the density of water.

## 5. Results

A computer code has been devised in order to perform the necessary simulations. All external inputs and other parameters range of variation have been imposed such that to ensure mechanical and geometrical stability. The external parameters are presented in Table 1. A first investigation was performed in order to assess the flow field pattern. Snapshots of the streamlines distribution have been plotted

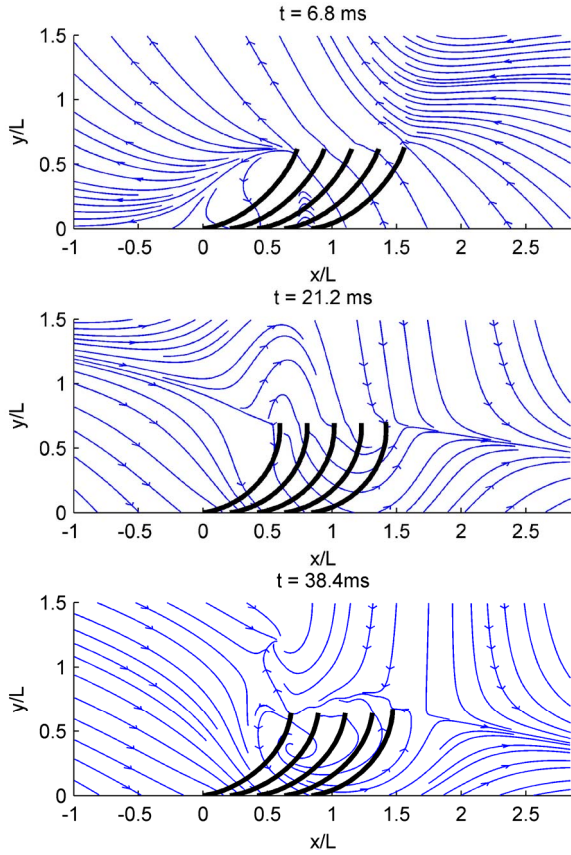


**Fig. 5.** Five cilia array streamlines distribution. Spacing 0.21.

in (Fig. 5) at different moments of time for a 5 cilia array configuration.

**Table 1.** External parameters

Parameter	L	a	q	f	
Value	100	1	10	25	0.001
Unit	m	m	m	Hz	Ns/m <sup>2</sup>
Parameter	E	B <sub>x</sub> =B <sub>y</sub>	w		0
Value	10 <sup>6</sup>	0.01	1000		4 · 10 <sup>-7</sup>
Unit	Pa	T	kg/m <sup>3</sup>		H/m

As a general trend, fluid flows from right to left over one 40 ms cycle, but there are instants when a flow reversal is observed. On the other hand there is some amount of fluid that crosses the top boundary of domain. Also, a consistent vortex is noticeable at several moments over the cycle covering the central area swept by cilia. We conclude that, in the semi-infinite domain, an array of cilia can work both as a tool for fluid transportation

along x-axis and as a tool for mixing transportation along x-axis and as a tool for mixing. In order to distinguish which feature is

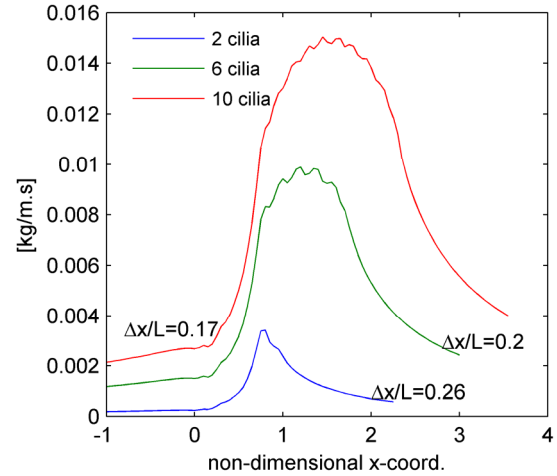


**Fig. 6.** Averaged x-mass flow rate for different configurations.

prevailing on average and in what amount, we can define the transportation efficiency as

$$\mathcal{E}_T = \frac{\overline{\dot{m}_x^L}}{\overline{\dot{m}_x^R}} \quad \overline{\dot{m}_x} = \frac{1}{t} \int_0^t \dot{m}_x(\tau) d\tau \quad (18)$$

where superscripts L and R stand for left and right boundaries of the computational domain. The time averaged x-mass flow rate versus x-coordinate for several configurations and minimum spacing is plotted in (Fig. 6) The minimum spacing is determined such that mechanical and geometrical equilibrium is ensured. The maximum mass boundary is attained for the minimum spacing corresponding to the configurations considered is illustrated in (Fig. 7). The efficiency  $\mathcal{E}$  depends on the spacing among cilia  $\Delta x / L$  and the number of cilia in array.

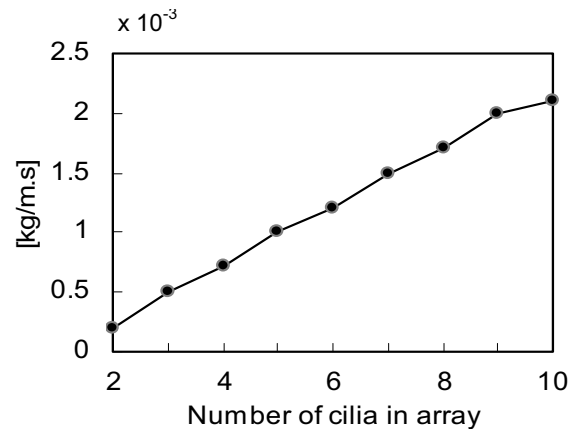


**Fig. 7.** Maximum x-mass flow rate.

## 6. Conclusions

Rotating magnetic field is a viable possibility for actuating a battery of cilia in order to produce fluid transportation even in a semi infinite domain. We expect better performance in a confined geometry. Beside number, cilia spacing is a crucial parameter that influences mass flow rate. Odd kinematic behavior is noticed for the first cilium in the array closest to the inlet boundary (on a time averaged basis).

## Acknowledgements

This work has been supported through grant ARTIC FP6-2004-NMP-TI4.

## 7. References

- [1] Gueron, S., Liron, N., "Ciliary motion modeling and dynamic multicilia interactions". *Biophys. J.*, 63, pp. 1045-1058, 1992
- [2] Gueron, S., Levit-Gurevich, K., Liron, N., Blum, J.J., "Cilia internal mechanism and metachronal coordination as the result of hydrodynamical coupling", *Proc. Natl. Acad. Sci. USA*, 94, pp 6001-6006, *Applied Mathematics*, 1997
- [3] Gueron, S., Levit-Gurevich, K., "Computation of the internal forces in cilia: Application to ciliary motion, the effects of viscosity and interactions", *Biophys. J.*, 74, pp. 1658-1676, 1998
- [4] Gueron, S., Levit-Gurevich, "Energetic considerations of ciliary beating and the advantage of metachronal coordination", *Proc. Natl. Acad. Sci. USA*, 96, no 2, pp 12240-12245, *Applied Mathematics*, 1999
- [5] Isvoranu, D., Ioan, D., Parvu, P., "Numerical simulation of single artificial cilium magnetic driven motion in a semi-infinite domain", *Proceedings of the 1st European Conference on Microfluidics, Microfluidics 2008 - Bologna*, pp. 226, 2008
- [6] D. Ioan, I.F. Hantila, M. Rebican, C. Constantin, "FLUXSET Sensor Analysis based on nonlinear magnetic wire model of the core", *Electromagnetic Nondestructive Evaluation (II)*, pp. 160-169, IOS Press, Amsterdam 1998.
- [7] Artic home page: Available: <http://www.hitech-projects.com/euprojects/artic>
- [8] Jackson, J.D., "Classical Electrodynamics", John Wiley & Sons. , 1974